



## Facile fabrication of well-defined hydrogel beads with magnetic nanocomposite shells

Hongxia Liu<sup>a</sup>, Chaoyang Wang<sup>a,\*</sup>, Quanxing Gao<sup>a</sup>, Jianxin Chen<sup>b</sup>,  
Biye Ren<sup>a</sup>, Xinxing Liu<sup>a</sup>, Zhen Tong<sup>a,\*</sup>

<sup>a</sup> Research Institute of Materials Science, South China University of Technology, Guangzhou 510640, China

<sup>b</sup> College of Veterinary Medicine, South China Agricultural University, Guangzhou 510640, China

### ARTICLE INFO

#### Article history:

Received 2 December 2008

Received in revised form 21 April 2009

Accepted 22 April 2009

Available online 3 May 2009

#### Keywords:

Alginate hydrogel bead

Magnetic nanoparticle

Core-shell structure

Self-assembly

Nanocomposite

### ABSTRACT

Well-defined magnetic nanocomposite beads with alginate gel cores and shells of iron oxide ( $\gamma$ - $\text{Fe}_2\text{O}_3$ ) nanoparticles were prepared by self-assembly of colloidal particles at liquid–liquid interfaces and subsequent in situ gelation.  $\text{Fe}_2\text{O}_3$  nanoparticles could spontaneously adsorb onto the water droplet surfaces to stabilize water-in-hexane emulsions. Water droplets containing sodium alginate were in situ gelled by calcium cations, which were released from calcium-ethylenediamine tetraacetic acid (Ca-EDTA) chelate by decreasing pH value through slow hydrolysis of D-glucono- $\delta$ -lactone (GDL). The resulting hybrid beads with a core–shell structure were easily collected by removing hexane. This facile and high efficient fabrication had a 100% yield and could be carried out at room temperature. Insulin microcrystal was encapsulated into the hybrid beads by dispersing them in the aqueous solution of alginate sodium in the fabrication process. The sustained release could be obtained due to the dual barriers of the hydrogel core and the close-packed inorganic shell. The release curves were nicely fitted by the Weibull equation and the release followed Fickian diffusion. The hybrid beads may find applications as delivery vehicles for biomolecules, drugs, cosmetics, food supplements and living cells.

© 2009 Elsevier B.V. All rights reserved.

### 1. Introduction

Hydrogels with a reversible volume response to external stimuli have been studied extensively as biomaterials for tissue engineering and cell encapsulation, and as carriers of drugs, peptides or proteins, due to their hydrophilic character and possible biocompatibility (Peppas and Langer, 1994; Lee and Mooney, 2001; Osada et al., 1992; Hoffman, 2002). Over the last few years, artificial conjugation of hydrogels and inorganic components has received increasing attention due to the synergistic properties between hydrogels and inorganic components (Schnepp et al., 2006; Ogomi et al., 2005; Qiu and Park, 2001; Liang et al., 2007; Ribeiro et al., 2004; Wang et al., 2008; Hantzschel et al., 2007). In particular, hydrogel-based hybrid composites incorporating colloidal inorganic particles could be designed with tailored mechanical and functional properties, and have many important uses in bioseparation, biomedical, catalytic applications (Ogomi et al., 2005; Qiu and Park, 2001; Liang et al., 2007; Ribeiro et al., 2004). To date, a number of approaches for the preparation of these hybrid hydrogels have been suggested and developed. They can be divided into four kinds

basically. The first one is the incorporation of preformed inorganic particles into the hydrogel matrix by mixing and subsequent in situ gelation (Ribeiro et al., 2004; Wang et al., 2008). The second one is the deposition of inorganic particles into the preformed hydrogel matrix by the in situ mineralization (Ogomi et al., 2005; Liang et al., 2007). The third one is coupling both preformed inorganic particles and hydrogel matrix together (Hantzschel et al., 2007). The possible fourth one is the simultaneous formation of both hydrogel matrix and inorganic particles in the reaction system. Although commonly used, these classical methods have a limit that inorganic particles randomly distribute in the hydrogel matrix. New, better controlled synthetic routes towards such hybrid materials are eagerly anticipated.

Recently, self-assembly of colloidal particles at liquid–liquid interfaces has been well documented and offers a straightforward pathway for the production of organized nanostructures (Aveyard et al., 2003). In this approach, colloidal particles spontaneously localize at the interface to minimize the helmholtz free energy. Typically, so-called Pickering emulsion is stabilized and novel microcapsules known as colloidosomes whose shells consist of colloid particles have been created using this strategy (Binks et al., 2005; Velev et al., 1996; Dinsmore et al., 2002; Lin et al., 2003; Yow and Routh, 2006; Chen et al., 2007; Laib and Routh, 2008). Noble et al. (2004) and Cayre et al. (2004) produced colloidosome hydrogel beads with agarose gel cores and shells of polymer particles

\* Corresponding authors. Tel.: +86 20 87112886; fax: +86 20 87112886.

E-mail addresses: [zhywang@scut.edu.cn](mailto:zhywang@scut.edu.cn) (C. Wang), [mctzong@scut.edu.cn](mailto:mctzong@scut.edu.cn) (Z. Tong).

by self-assembly of colloid particles at liquid–liquid interfaces and subsequent gelation of the aqueous cores. Duan et al. (2005) prepared magnetic colloidosome hydrogel beads with agarose gel cores and shells of inorganic particles based on interfacial self-assembly of  $\text{Fe}_3\text{O}_4$  nanoparticles. Therefore, well-defined hydrogel beads with shells of inorganic particles can be easily obtained by interfacial self-assembly of inorganic particles. However, agarose gelation needs thermal treatment ( $\geq 70^\circ\text{C}$ ) which can limit the tenability and applicability of this method. Most recently, we have successfully prepared colloidosome hydrogel beads with alginate gel cores and shells of porous  $\text{CaCO}_3$  microparticles by self-assembly of colloidal particles at liquid–liquid interfaces and subsequent in situ gelation at room temperature (Wang et al., 2007; Liu et al., 2008).

Colloidosome hydrogel beads have many advantages in encapsulation: emulsification provides a simple method of preparing gel beads from a wide variety of fluids and with controlled sizes ranging from submicrometer to several millimeters. Active substances can be loaded efficiently with minimal loss because of complete separation of the internal and external fluids in the fabrication process. The various colloidal particles are suitable for this fabrication strategy to endow gel beads with versatile functions. The hydrogel beads are around with a close-packed shell of colloidal particles and the interstices between the particles form an array of uniform pores whose size is easily adjusted over the nanometer to micrometer scale to control the permeability (Dinsmore et al., 2002). Therefore, colloidosome hydrogel beads may find applications as a new kind of delivery vehicles for biomolecules, drugs, cosmetics, food supplements and living cells. However, a high efficient preparation of colloidosome beads is still a challenge. Meanwhile, to the authors' best knowledge, colloidosome beads as drug deliveries are not reported up to date.

In this work, we demonstrate the first example of the application of colloidosome beads as a drug delivery system. Magnetic colloidosome beads with alginate gel cores containing drug and shells of  $\gamma\text{-Fe}_2\text{O}_3$  nanoparticles are facilely and high efficiently produced by self-assembly of colloid particles at liquid–liquid interfaces and subsequent in situ gelation at room temperature with a 100% yield. Alginate is a well-known biomaterial obtained from brown algae and is widely used for drug delivery and in tissue engineering due to its biocompatibility, low toxicity, relatively low cost, and simple gelation with divalent cations such as  $\text{Ca}^{2+}$  (Lu et al., 2005). Three features make the fabricated hybrid colloidosome capsules of specific interest and significance (Yow and Routh, 2006; Koo et al., 2006). First, they are superparamagnetic and can be manipulated by external magnetic fields. Second, their gel cores can be reversibly filled with water by osmotic swelling and drying. Third, dual levels of encapsulation with gelled core and particle shell are obtained. Herein, insulin microcrystal, as a model drug, is loaded into the colloidosome beads by dispersing in water phase during the colloidosome fabrication process. The release behavior of the drug-loaded colloidosomes is investigated.

## 2. Materials and methods

### 2.1. Materials

Sodium alginate (Kimitsu Chemical Industries Co., Japan, Mw 120,000) was dialyzed and freeze-dried before use. D-Glucono- $\delta$ -lactone (GDL, Sigma), insulin microcrystals (Sigma) were used as received. Calcium-ethylenediamine tetraacetic acid (Ca-EDTA) chelate (Standard reagent, Tianjin Institute for Chemicals, China), iron (II) chloride tetrahydrate ( $\text{FeCl}_2 \cdot 4\text{H}_2\text{O}$ ), iron (III) chloride hexahydrate ( $\text{FeCl}_3 \cdot 6\text{H}_2\text{O}$ ), 2-propanol (HPLC grade), concentrated ammonia, oleic acid, *n*-hexane, ethanol, rhodamine B (Guangzhou Chemical Factory, China) were used without further purification.

Water used in all experiments was purified by deionization and filtration with a Millipore purification apparatus to the resistivity higher than  $18.0\text{ M}\Omega\text{ cm}$ .

### 2.2. Preparation of $\gamma\text{-Fe}_2\text{O}_3$ nanoparticles capped with oleic acid

Iron oxide ( $\gamma\text{-Fe}_2\text{O}_3$ , maghemite) magnetic nanoparticles (MPs) were synthesized using methods similar to that used by Koo et al. (2006). A 0.5 g portion of  $\text{FeCl}_3 \cdot 6\text{H}_2\text{O}$  was added to 50 mL of nitrogen-purged HPLC grade 2-propanol. Then, 0.25 g of  $\text{FeCl}_2 \cdot 4\text{H}_2\text{O}$  was added while the solution was continuously stirred. The solution color was yellowish-orange after complete dissolution of the iron precursors. Then, the solution temperature was gradually raised to  $50^\circ\text{C}$  and concentrated aqueous ammonia was added to the solution in excess,  $<10\text{ mL}$ . The color of the solution changed to dark brown after 15 min of continuous stirring. To speed up the precipitation of the MPs, the resulting solution was placed in a refrigerator for 5 h. The MPs were subsequently washed with methanol 3 times and settled by centrifugation at 10,000 rpm for 5 min. A 10 mM oleic acid solution, in 50 mL methanol, was then added to the MPs, and this mixture was stirred for 3 h. After completing the synthesis, the maghemite MPs were thoroughly washed with methanol to remove excess oleic acid and finally were dispersed in 50 mL hexane. This MPs suspension was used as synthesized. The resulting oleic acid-stabilized maghemite MPs were single crystalline and uniform with diameters of  $\sim 5\text{ nm}$  (see Fig. 1).

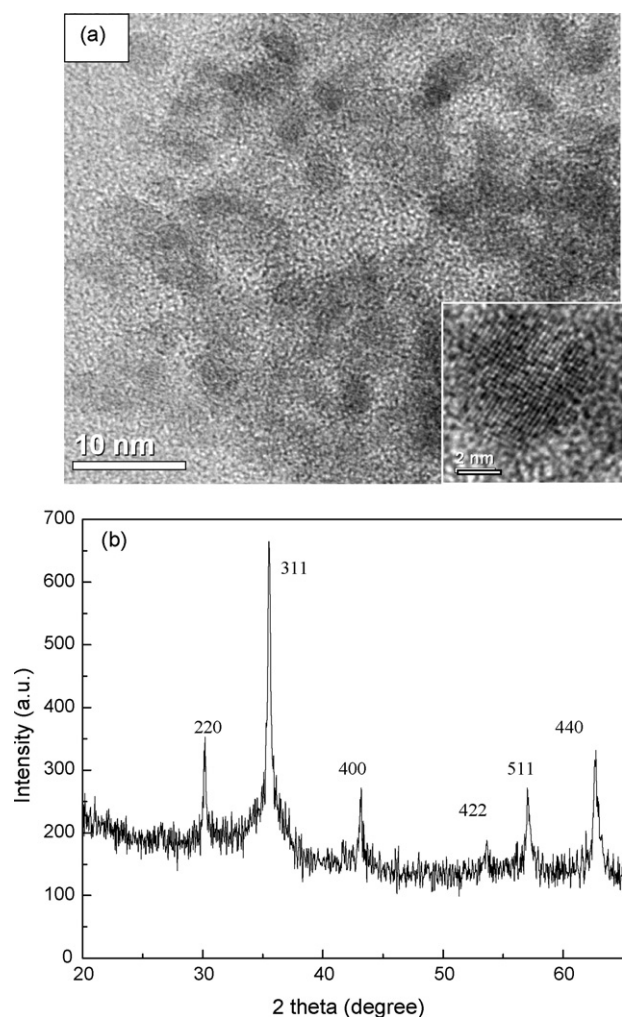


Fig. 1. (a) TEM images and (b) XRD pattern of  $\text{Fe}_2\text{O}_3$  magnetic nanoparticles (MPs) capped with oleic acid.

### 2.3. Fabrication of magnetic colloidosome beads

In a typical fabrication, sodium alginate (10 mg), Ca-EDTA aqueous solution (100  $\mu$ L, 6 wt%) and water (350  $\mu$ L) were mixed at magnetic stirring. Then, freshly prepared GDL aqueous solution (50  $\mu$ L, 0.25 g/mL) was added into and the mixture was stirred for seconds. The solution was rapidly added into 2 mL hexane with MPs (1 wt%) and the system was shaken for 2 h for alginate gelation. Then, most hexane was decanted. After the complete evaporation of remnant hexane at room temperature, magnetic colloidosome beads with alginate gel cores and shells of MPs were obtained.

### 2.4. Drug loading and in vitro release

Drug-loaded colloidosome beads were fabricated in the same way as described above except that sodium alginate aqueous solution contained insulin microcrystals (1 mg) in the colloidosome fabrication process. Insulin microcrystals of poor water-solubility were dispersed in the sodium alginate aqueous solution by stirring and ultrasonication. For comparison, insulin-loaded pure alginate gel spheres with the similar size were prepared in the similar way to that for the preparation of insulin-loaded colloidosome beads except that oleic acid was used as the stabilizer not Fe<sub>2</sub>O<sub>3</sub> nanoparticles.

For release study, the supernatant solution was collected from 3 mL suspension of the insulin-loaded colloidosome beads or pure alginate gel beads at different pH values (adjusted with sodium hydroxide or hydrochloric acid) by centrifuging after desired dipping intervals. The released quantity of insulin was estimated upon the UV spectroscopy intensity at 276 nm. This release was persisted until the insulin quantity in the supernatant became undetectable. In order to determine the unreleased insulin quantity in the beads, the hydrogel beads were treated repeatedly with acid and ultrasonication after the release test. All supernatant solutions after centrifugation were collected and the unreleased quantity of insulin in the hydrogel beads was evaluated with UV spectroscopy intensity. The in vitro release was performed with continuous shaking at 37 °C.

### 2.5. Characterization

Transmission electron microscopy (TEM) observation was conducted on a JEM-2010HR electron microscopy (JEOL Ltd., Japan). The sample was prepared by placing 10  $\mu$ L magnetic nanoparticles ethanol dispersion on a carbon-coated copper grid. The observation was carried out under accelerating voltages of 200 kV. X-ray diffraction of the magnetic nanoparticles was performed in transmission geometry using an X'pert PRO diffractometer (40 kV and 40 mA) equipped with Cu K $\alpha$  source (wavelength  $\lambda$  = 0.154 nm) at room temperature. The wet colloidosome beads were observed with an optical microscope (Carl Zeiss, German). The confocal micrograph was taken with a Leica TCS-SP2 confocal laser scanning microscope (CLSM) with a 20 $\times$  objective with a numerical aperture of 1.4 at excitation wavelength of 543 nm. The colloidosome beads were dispersed in water containing rhodamine B for CLSM testing. The morphology of dry colloidosome beads was observed by scanning electron microscopy (SEM) with a Philips XL 30 at the acceleration voltage of 15 kV. Samples were prepared by dropping the colloidosome suspension on a quartz wafer, dried overnight, then sputtered with gold. Magnetic characterization of the colloidosome beads and Fe<sub>2</sub>O<sub>3</sub> nanoparticles were performed on a Quantum Design (MPMS XL-7) magnetometer. UV absorbance of insulin was recorded with a Hitachi U-3010 UV-vis spectrophotometer.

## 3. Results and discussion

### 3.1. Fabrication of magnetic nanocomposite colloidosome beads

In our previous work, we have fabricated alginate gel beads with shells of porous CaCO<sub>3</sub> microparticles by self-assembly of colloidal particles at liquid–liquid interfaces and subsequent in situ gelation at room temperature (Wang et al., 2007; Liu et al., 2008). In a typical fabrication, porous CaCO<sub>3</sub> microparticles were dispersed in sunflower oil. Aqueous solution of sodium alginate was added into sunflower oil and water-in-oil emulsion was formed by stirring. Freshly prepared GDL aqueous solution was added into the resulting water-in-oil emulsion stabilized by particles to gel the aqueous alginate core. After 3 times of wash with ethanol to remove sunflower oil, hybrid hydrogel beads with shells of inorganic particles were obtained. The yield of the intact colloidosome beads by this method was low (about 60%). The reasons are that adding GDL into the emulsion to gel the aqueous alginate core will lightly destroy the performed water-in-oil emulsion and some colloidosome beads will be distorted in the washing process with ethanol to remove sunflower oil. In this work, we want to enhance the yield of the intact hybrid colloidosome beads. The fabrication strategy is illustrated in Fig. 2. An aqueous solution of sodium alginate, Ca-EDTA, GDL and drug microcrystals were rapidly emulsified in hexane with Fe<sub>2</sub>O<sub>3</sub> nanoparticles to produce water-in-oil emulsion by shaking and nanoparticles were self-assembled at liquid–liquid interfaces. The water droplets containing sodium alginate were in situ gelled by Ca<sup>2+</sup>, which was released from Ca-EDTA by decreasing pH through slow hydrolysis of GDL. The gelation process needed about 2 h. Then, most hexane was decanted. After the complete evaporation of remnant hexane, the drug-loaded hybrid colloidosome beads with shells of magnetic nanoparticles were obtained. Hexane was used as the oil phase due to its very low toxicity and easy removal by evaporation at room temperature. So washing for removing oil was not needed. All aqueous drops were converted to the hydrogel cores of the hybrid colloidosome beads. The fabrication process of magnetic hybrid colloidosomes could be carried out at room temperature to minimize heat effects on the bioactivity of encapsulated materials in the further applications. By our methodology, robust drug-loaded colloidosome beads can be easily prepared with a 100% yield, which is very important to produce in large quantity for industry.

### 3.2. Observation of colloidosome structure

We successfully fabricated the magnetic colloidosomes with alginate gel cores and shells of Fe<sub>2</sub>O<sub>3</sub> nanoparticles by self-assembly of colloidal particles at liquid–liquid interfaces and subsequent in situ gelation. Typical polar optical microscopy photos of the resultant colloidosomes in hexane and redispersed in water are shown in Fig. 3a and b, respectively. The colloidosomes are spherical, fine unique and can be redispersed in water appearing similarly to those dispersed in hexane. Alginate gel beads are obviously surrounded with thin, bright shells due to Fe<sub>2</sub>O<sub>3</sub> nanoparticles of single crystalline under polar lights as seen from Fig. 3b, which prove that the core–shell structure should be formed. The alginate gel core is important for the structural integrity of the colloidosomes. It gives the colloidosomes enough mechanical strength to the transfer into water, also helps to fix Fe<sub>2</sub>O<sub>3</sub> nanoparticles assembled on the interface. We find this structure of colloidosome is very stable in water after storage for more than 1 year.

However, the colloidosome may entirely collapse because of loss of water in alginate gel if we dry them in vacuum, which can be indicated by SEM images of the colloidosomes shown in Fig. 4a. Though the colloidosomes have collapsed, they still keep spherical shape.

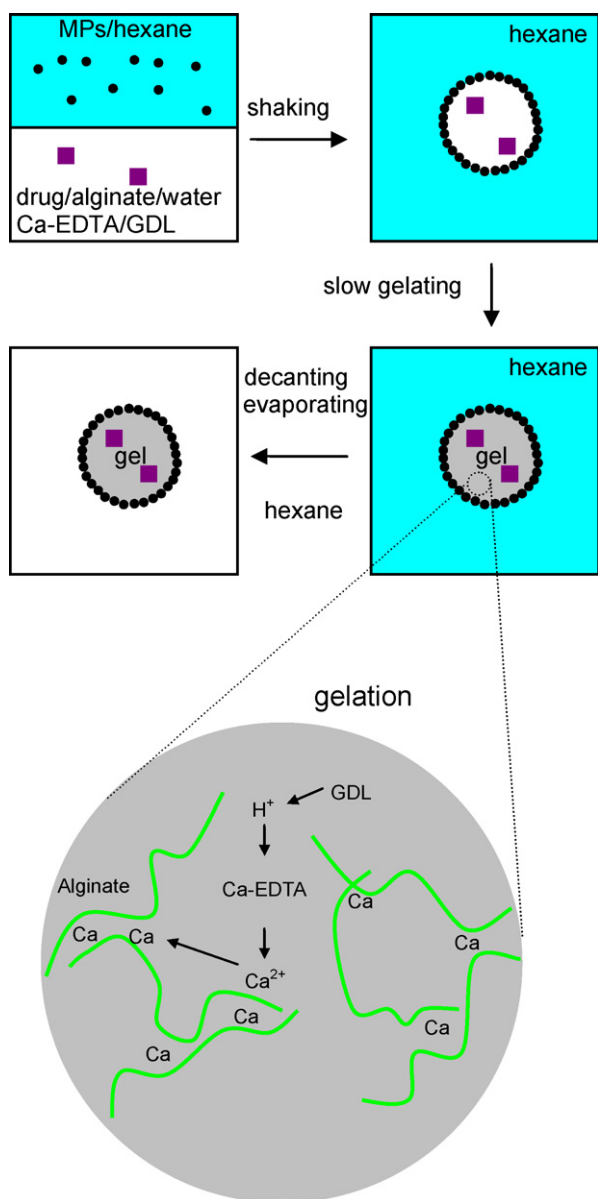


**Fig. 2.** Schematic illustration of the processes for preparing colloidosome based on self-assembled  $\gamma\text{-Fe}_2\text{O}_3$  magnetic nanoparticles (MPs) at the interface of the water droplet including 2 wt% alginate in  $n$ -hexane and gelation of sodium alginate.

A confocal fluorescence microscopy image of the colloidosome bead dispersed in rhodamine B aqueous solution is showed in Fig. 4b. The red luminescence is seen inside and outside the colloidosomes and the dark shells of  $\text{Fe}_2\text{O}_3$  nanoparticles are obviously observed. This result further proves that the colloidosomes with the alginate gel core and  $\text{Fe}_2\text{O}_3$  nanoparticles core are obtained. On the other hand, rhodamine B in the aqueous solution can diffuse into the colloidosome beads through the shell of  $\text{Fe}_2\text{O}_3$  nanoparticles, which is important to drug loading and release for the colloidosome beads.

### 3.3. Magnetic property of colloidosome beads

Magnetic hysteresis loops of  $\gamma\text{-Fe}_2\text{O}_3$  nanoparticles and the colloidosomes at 5 K and 300 K are presented in Fig. 5.  $\text{Fe}_2\text{O}_3$  nanoparticles and the colloidosomes are superparamagnetic at 300 K and a little hysteretic at 5 K. The saturation magnetization values at room temperature are 30 emu/g for  $\text{Fe}_2\text{O}_3$  nanoparticles and 2 emu/g for the colloidosomes, while the saturation magnetiza-

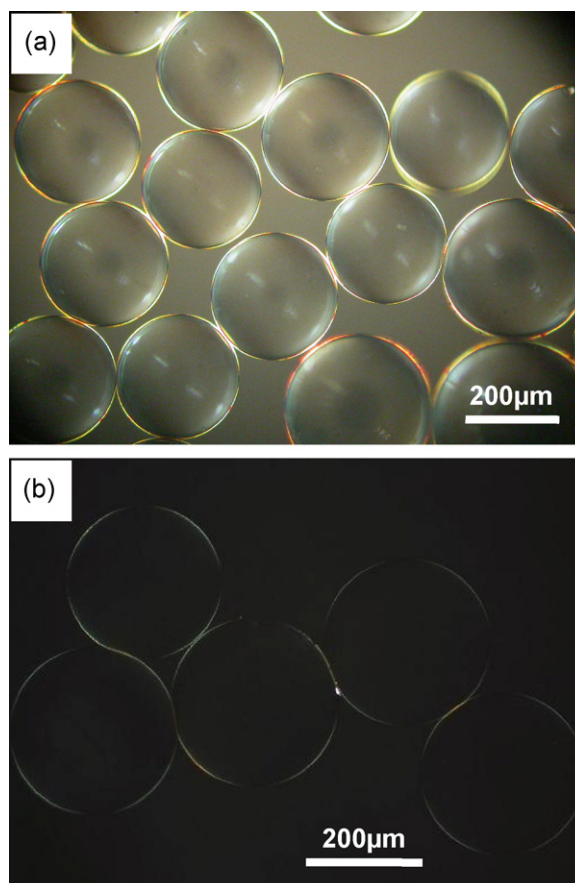


**Fig. 3.** Polar optical microscopy photos of the colloidosomes with  $\text{Fe}_2\text{O}_3$  nanoparticle shell and alginate gel core (a) in hexane with polarizer and analyzer at  $45^\circ$  and (b) in water with polarizer and analyzer at  $90^\circ$ .

tion values at 5 K are 40 emu/g for  $\text{Fe}_2\text{O}_3$  nanoparticles and 3 emu/g for the colloidosomes. Very low coercivity values were observed in the two samples (ca 200 Oe) and probably arise from the large agglomerates, the magnetic moment of which is blocked (Park et al., 2007). As the colloidosomes contain alginate gel core, they exhibit relatively small magnetization. However, a clear magnetic response is evident and the colloidosomes can readily be moved and collected with an external magnetic field, which is shown in Fig. 5c. The magnetic shells allow easy manipulation of the beads by magnetic fields.

### 3.4. In vitro release

Insulin is the most widely used protein drug, and is indispensable for the patients of the type I diabetes (Carino and Mathiowitz, 1999; Ye et al., 2006). The research on insulin delivery and release has attracted many interests, including oral insulin delivery (Carino and Mathiowitz, 1999). Insulin microcrystals as a drug model were loaded into the colloidosome beads by dispersing in the alginate aqueous solutions before gelation. After removal of hexane, the insulin-loaded hydrogel beads were stored in a close container. They could be easily redispersed in water and keep spherical after storage for more than a month. The release behavior of insulin crystals from the colloidosomes was investigated. The release profile at pH 1.2 is shown in Fig. 6 compared with those from insulin-loaded pure alginate gel spheres without  $\text{Fe}_2\text{O}_3$  nanoparticles shells and bare insulin crystals. Because of a fine solubility at pH 1.2, bare insulin crystals fast releases at pH 1.2 with the total release time of 60 s and the half release time of less than 30 s. Insulin release

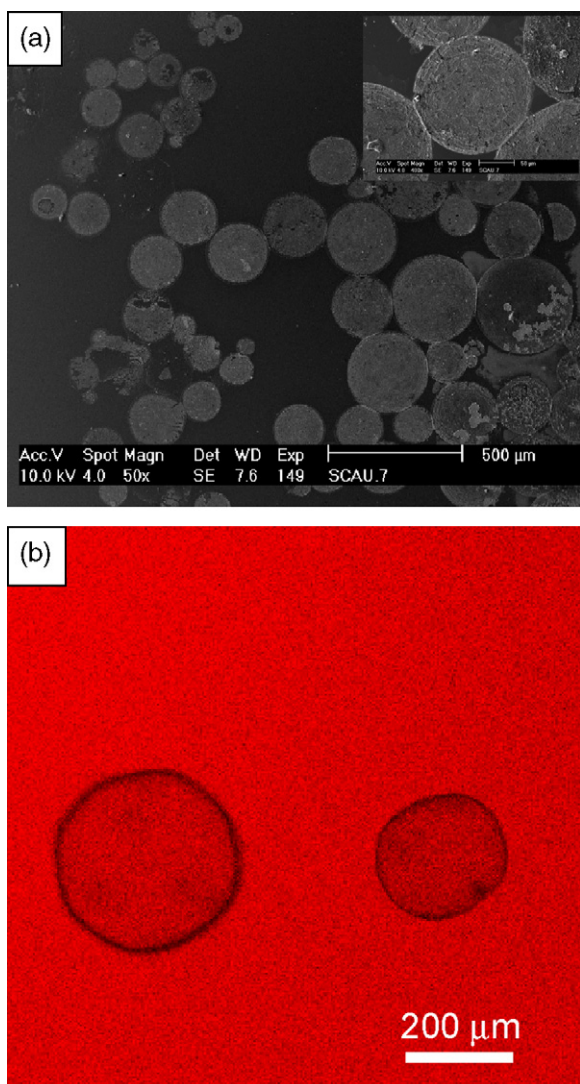


**Fig. 4.** SEM images of the dried colloidosomes (inset: high magnification SEM image) (a) and CLSM photos of the colloidosomes being dispersed in rhodamine B aqueous solution (b).

from both pure alginate gel spheres and the colloidosomes is much slower than bare insulin crystals. The half release time is 390 min for pure alginate gel spheres and 460 min for the colloidosomes. The release profile at pH 7.4 is presented in Fig. 7. The half release time is 1.5 h for bare insulin crystals, 9.4 h for pure alginate gel spheres and 17.9 h for the colloidosomes. The insulin release from pure alginate gel spheres is slower than that from bare insulin crystals at pH 7.4 and pH 1.2 due to encapsulation of hydrogel. Meanwhile, the insulin release from the colloidosome is slower than that from pure alginate gel spheres. The reason is that the close-packed shells of  $\text{Fe}_2\text{O}_3$  nanoparticles can block the diffusion of insulin from the alginate gel cores to the release medium. The colloidosomes have a dual controlled release mechanism of encapsulation of gel cores and block of nanoparticle shells.

In order to describe the kinetics of drug release and the discernment of the release mechanisms, we use the Higuchi law (Higuchi, 1961) and the Weibull equation (Van Vooren et al., 2001) to fit the curve of insulin crystals release from the colloidosome beads and pure alginate gel spheres. The Higuchi law indicates that the fraction of drug released is proportional to the square root of time:

$$\frac{M_t}{M_\infty} = kt^{1/2} \quad (1)$$

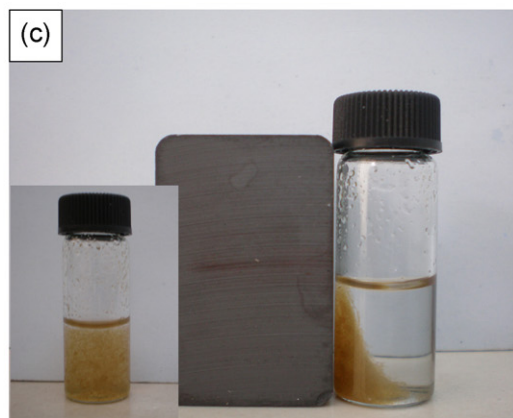
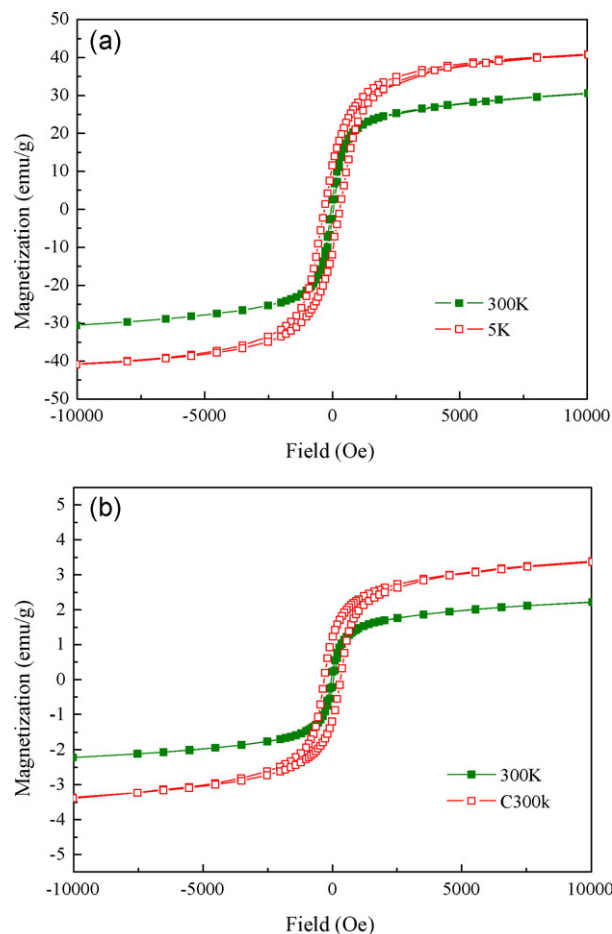


**Fig. 5.** Field-dependent magnetization curves of (a) the colloidosomes and (b) the synthesized  $\gamma\text{-Fe}_2\text{O}_3$  magnetic nanoparticles, and (c) is the photo of colloidosomes separation inside the container under an external magnetic field (inset: redispersion suspension).

where  $M_t/M_\infty$  is the fractional drug released at time  $t$ ,  $M_t$  and  $M_\infty$  are cumulative amounts of drug released at time  $t$  and infinite time, and  $k$  is a constant related to the formulation of loaded drug and release medium. The Weibull equation is expressed as:

$$\frac{M_t}{M_\infty} = 1 - \exp(-at^b) \quad (2)$$

where  $a$  and  $b$  are constants. Although this function is frequently applied to the analysis of dissolution and release studies, its empirical use has been criticized (Costa et al., 2001). Recently, Kosmidis et al. found that Eq. (2) describes nicely the entire drug release curve

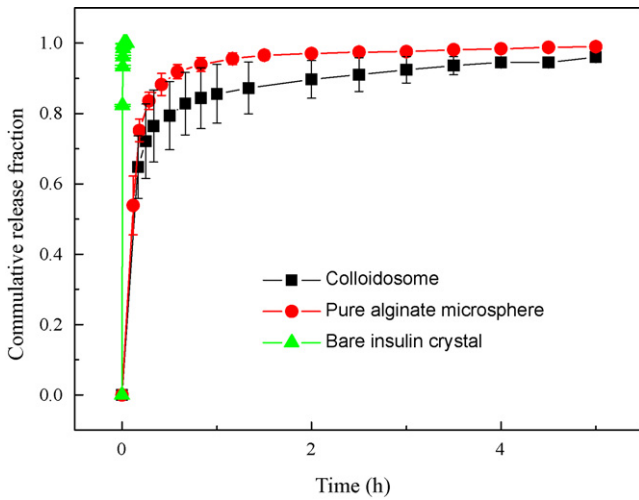


**Fig. 6.** Release curve at pH 1.2 of bare insulin microcrystal, the colloidosomes and alginate gel spheres loaded insulin microcrystal ( $n=3$ ).

of release from the spherical matrices (Kosmidis et al., 2003a,b). Here the Higuchi law can be predigested as:

$$F = kt^{1/2} \quad (3)$$

The Weibull equation can be expressed as:

$$\text{Ln Ln} \left( \frac{1}{1-F} \right) = b \text{Ln } t + \text{Ln } a \quad (4)$$

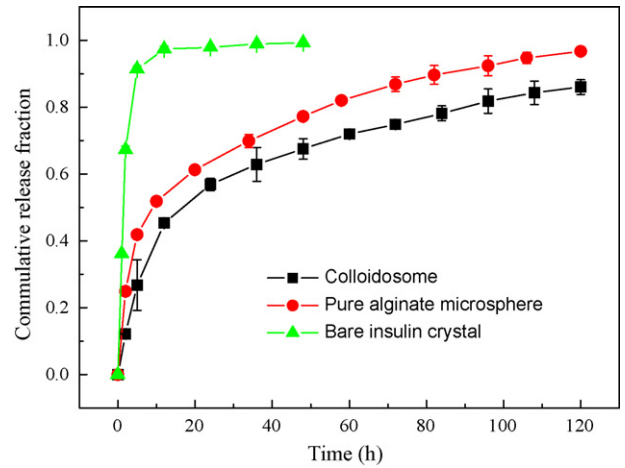


**Fig. 7.** Release curve at pH 7.4 of bare insulin microcrystal, the colloidosomes and alginate gel spheres loaded insulin microcrystal ( $n=3$ ).

where  $F$  is  $M_t/M_\infty$ , the fractional drug released at time  $t$ . We fit the insulin crystals release curves for the colloidosome beads and the pure alginate gel spheres at pH 1.2 and pH 7.4 using Eqs. (3) and (4). The value of  $r$  which is the correlation coefficient of the linear regressions is listed in Table 1. From Table 1, we can see that the values of  $r$  derived from the linear regressions of the Weibull equation are very close and larger than that from the linear regressions of the Higuchi equation. Thus the Weibull equation can better fit the insulin crystals release curves. The good fitting curves and regression lines by Eq. (4) to the releases from the colloidosome beads and

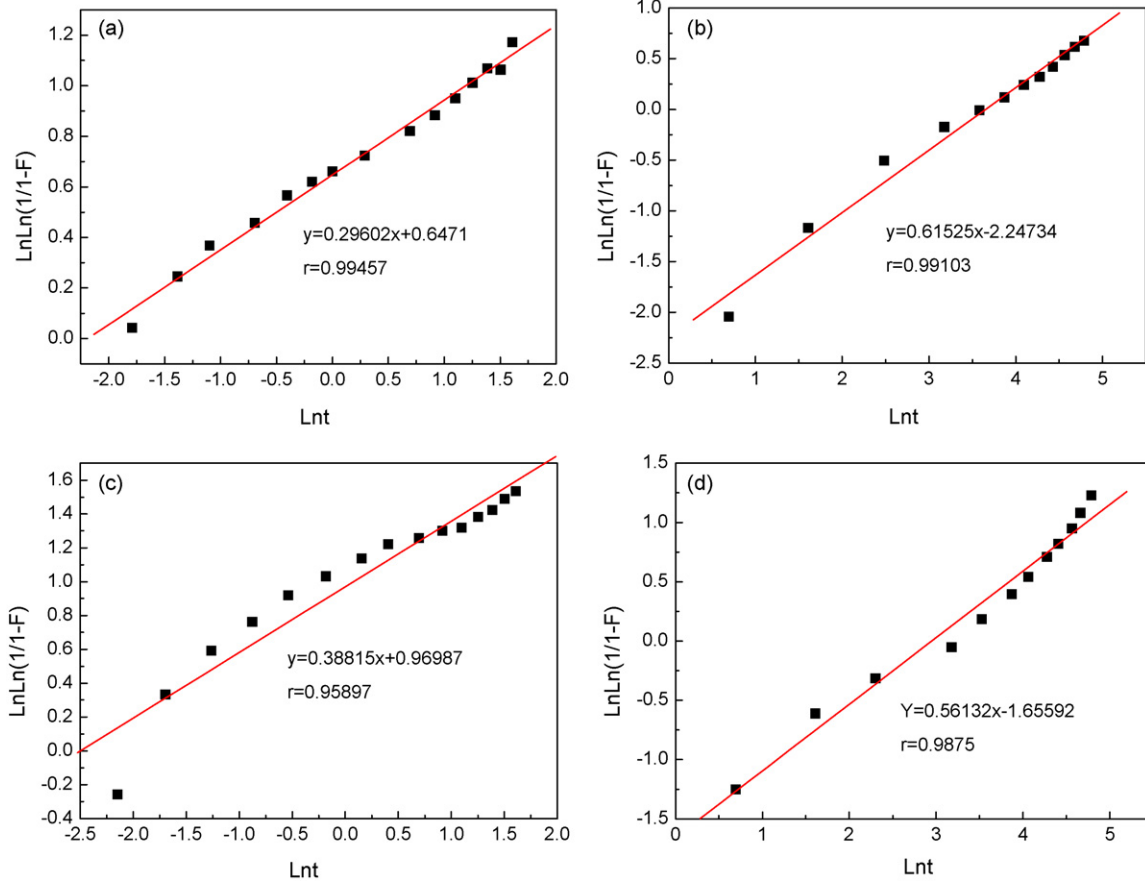


**Fig. 8.** The fitting regression line by Weibull equation for insulin crystals release from the colloidosomes at pH 1.2 (a), pH 7.4 (b), and from the pure alginate gel spheres at pH 1.2 (c) and pH 7.4 (d).

**Table 1**

The correlation coefficient of the linear regressions of fitting release curves by Higuchi and Weibull models.

Model	Colloidosome beads		Pure alginate gel spheres	
	pH 1.2	pH 7.4	pH 1.2	pH 7.4
Higuchi	0.744	0.973	0.707	0.970
Weibull	0.995	0.9919	0.959	0.988

the pure alginate gel spheres at pH 1.2 and pH 7.4 are shown in Fig. 8. We know that the slope of the regression line of Eq. (4) is the constant  $b$  of Weibull equation. From Fig. 8,  $b$  for the colloidome beads and the pure alginate gel spheres at pH 1.2 is 0.30 and 0.39, respectively.  $b$  for the colloidome beads and the pure alginate gel spheres at pH 7.4 is 0.62 and 0.56, respectively. Kosmidis et al. concluded that Weibull equation arises from the creation of a concentration gradient near the releasing boundaries of the Euclidian matrix or because of the “fractal kinetics” behavior associated with the fractal geometry of the environment (Papadopoulou et al., 2006). They also summarized the diffusional mechanism in connection with the specific  $b$  values of Weibull equation and concluded that for values of  $b$  lower than 0.75 the release follows Fickian diffusion and for Fickian diffusion the increase of  $b$  reflects the decrease of the disorder of the medium. As the Section 3, Weibull equation can nicely fit the insulin release curves and the release follows Fickian diffusion.

#### 4. Conclusions

In this study, well-defined magnetic nanocomposite colloidosomes with alginate gel cores and shells of  $\text{Fe}_2\text{O}_3$  nanoparticles were facilely prepared by self-assembly of colloidal particles at liquid–liquid interfaces and subsequent in situ gelation with a 100% yield, which is promising to produce in large quantity for industry. The obtained colloidosomes can demonstrate an inherent magnetic response due to the presence of magnetic  $\text{Fe}_2\text{O}_3$  nanoparticles. The colloidosome can find applications in drug delivery, as well as microreactors, because the microcapsules can be filled with drug or reagent and treated with a magnetic field to target area. The colloidosomes have a dual-controlled insulin release mechanism of encapsulation of gel cores and block of nanoparticle shells. The release curve can be nicely fitted by the Weibull equation and the release follows Fickian diffusion.

#### Acknowledgments

This work was supported by the National Natural Science Foundation of China (20574023 and 20874030), the Scientific and Technologic Program of Guangzhou Municipality (2007J1-C0351) and NCET-07-0306.

#### References

Aveyard, R., Binks, B.P., Clint, J.H., 2003. Emulsions stabilised solely by colloidal particles. *Adv. Colloid Interface Sci.* 100–102, 503–546.  
 Binks, B.P., Murakami, R., Armes, S.P., Fujii, S., 2005. Temperature-induced inversion of nanoparticle-stabilized emulsions. *Angew. Chem. Int. Ed.* 44, 4795–4798.  
 Carino, G.P., Mathiowitz, E., 1999. Oral insulin delivery. *Adv. Drug Deliv. Rev.* 35, 249–257.  
 Cayre, O.J., Noble, P.F., Paunov, V.N., 2004. Fabrication of novel colloidosome microcapsules with gelled aqueous cores. *J. Mater. Chem.* 14, 3351–3355.  
 Chen, T., Colver, P.J., Bon, S.A.F., 2007. Organic–inorganic hybrid hollow spheres prepared from  $\text{TiO}_2$ -stabilized pickering emulsion polymerization. *Adv. Mater.* 19, 2286–2289.

Costa, P., Manuel, J., Lobo, S., 2001. Modeling and comparison of dissolution profiles. *Eur. J. Pharm. Sci.* 13, 123–133.  
 Dinsmore, A.D., Hsu, M.F., Nikolaidis, M.G., Marquez, M., Bausch, A.R., Weitz, D.A., 2002. Colloidosomes: selectively permeable capsules composed of colloidal particles. *Science* 298, 1006–1009.  
 Duan, H.W., Wang, D.Y., Sobal, N.S., Giersig, M., Kurth, D.G., Möhwald, H., 2005. Magnetic colloidosomes derived from nanoparticle interfacial self-assembly. *Nano Lett.* 5, 949–952.  
 Hantzschel, N., Zhang, F.B., Eckert, F., Pich, A., Winnik, M.A., 2007. Poly(N-vinylcaprolactam-co-glycidyl methacrylate) aqueous microgels labeled with fluorescent  $\text{LaF}_3:\text{Eu}$  nanoparticles. *Langmuir* 23, 10793–10800.  
 Higuchi, T., 1961. Rate of release of medicaments from ointment bases containing drugs in suspension. *J. Pharm. Sci.* 50, 874–875.  
 Hoffman, S., 2002. Hydrogels for biomedical applications. *Adv. Drug Deliv. Rev.* 54, 3–12.  
 Koo, H.Y., Chang, S.T., Choi, W.S., Park, J.H., Kim, D.Y., Velev, O.D., 2006. Emulsion-based synthesis of reversibly swellable, magnetic nanoparticle-embedded polymer microcapsules. *Chem. Mater.* 18, 3308–3313.  
 Kosmidis, K., Argyrakos, P., Macheras, P., 2003a. A reappraisal of drug release laws using Monte Carlo simulations: the prevalence of the Weibull function. *Pharm. Res.* 20, 988–995.  
 Kosmidis, K., Argyrakos, P., Macheras, P., 2003b. Fractal kinetics in drug release from finite fractal matrices. *J. Chem. Phys.* 119, 6373–6377.  
 Laib, S., Routh, A.F., 2008. Fabrication of colloidosomes at low temperature for the encapsulation of thermally sensitive compounds. *J. Colloid Interface Sci.* 317, 121–129.  
 Lee, K.Y., Mooney, D.J., 2001. Hydrogels for tissue engineering. *Chem. Rev.* 101, 1869–1879.  
 Liang, Y.Y., Zhang, L.M., Jiang, W., Li, W., 2007. Embedding magnetic nanoparticles into polysaccharide-based hydrogels for magnetically assisted bioseparation. *ChemPhysChem* 8, 2367–2372.  
 Lin, Y., Skaff, H., Böker, A., Dinsmore, A.D., Emrick, T., Russell, T.P., 2003. Nanoparticle assembly and transport at liquid–liquid interfaces. *Science* 299, 226–229.  
 Liu, H.X., Wang, C.Y., Gao, Q.X., Liu, X.X., Tong, Z., 2008. Fabrication of novel core–shell hybrid alginate hydrogel beads. *Int. J. Pharm.* 351, 104–112.  
 Lu, L., Liu, X.X., Dai, L., Tong, Z., 2005. Difference in concentration dependence of relaxation critical exponent  $n$  for alginate solutions at sol–gel transition induced by calcium cations. *Biomacromolecules* 6, 2150–2156.  
 Noble, P.F., Cayre, O.J., Alargova, R.G., Velev, O.D., Paunov, V.N., 2004. Fabrication of “hairy” colloidosomes with shells of polymeric microrods. *J. Am. Chem. Soc.* 126, 8092–8093.  
 Ogomi, D., Serizawa, T., Akashi, M., 2005. Controlled release based on the dissolution of a calcium carbonate layer deposited on hydrogels. *J. Control. Release* 103, 315–323.  
 Osada, Y., Okuzaki, H., Hori, H., 1992. Polymer gel with electrically driven motility. *Nature* 355, 242–244.  
 Papadopoulou, V., Kosmidis, K., Vlachou, M., Macheras, P., 2006. On the use of the Weibull function for the discernment of drug release mechanisms. *Int. J. Pharm.* 309, 44–50.  
 Park, K., Liang, G., Ji, X.J., Luo, Z.P., Li, C., Croft, M.C., Markert, J.T., 2007. Structural and magnetic properties of gold and silica doubly coated  $\gamma\text{-Fe}_2\text{O}_3$  nanoparticles. *J. Phys. Chem. C* 111, 18512–18519.  
 Peppas, N.A., Langer, R., 1994. New challenges in biomaterials. *Science* 263, 1715–1720.  
 Qiu, Y., Park, K., 2001. Environment-sensitive hydrogels for drug delivery. *Adv. Drug Deliv. Rev.* 53, 321–339.  
 Ribeiro, C.C., Barrias, C.C., Barbosa, M.A., 2004. Calcium phosphate–alginate microspheres as enzyme delivery matrices. *Biomaterials* 25, 4363–4373.  
 Schnepf, Z.A.C., Gonzalez-McQuire, R., Mann, S., 2006. Hybrid biocomposites based on calcium phosphate mineralization of self-assembled supramolecular hydrogels. *Adv. Mater.* 18, 1869–1872.  
 Van Vooren, L., Krikilion, G., Rosier, J., De Spiegeleer, B., 2001. A novel bending point criterion for dissolution profile interpretation. *Drug Dev. Ind. Pharm.* 27, 885–892.  
 Velev, O.D., Furusawa, K., Nagayama, K., 1996. Assembly of latex particles by using emulsion droplets as templates. 1. Microstructured hollow spheres. *Langmuir* 12, 2374–2384.  
 Wang, C.Y., Liu, H.X., Gao, Q.X., Liu, X.X., Tong, Z., 2007. Facile fabrication of hybrid colloidosomes with alginate gel cores and shells of porous  $\text{CaCO}_3$  microparticles. *ChemPhysChem* 8, 1157–1160.  
 Wang, C.Y., Liu, H.X., Gao, Q.X., Liu, X.X., Tong, Z., 2008. Alginate–calcium carbonate porous microparticle hybrid hydrogels with versatile drug loading capabilities and variable mechanical strengths. *Carbohydr. Polym.* 71, 476–480.  
 Ye, S.Q., Wang, C.Y., Liu, X.X., Tong, Z., Ren, B.Y., Zeng, F., 2006. New loading process and release properties of insulin from polysaccharide microcapsules fabricated through layer-by-layer assembly. *J. Control. Release* 112, 79–87.  
 Yow, H.N., Routh, A.F., 2006. Formation of liquid core–polymer shell microcapsules. *Soft Matter* 2, 940–949.